

# Unravelling concurring degradation mechanisms in InGaAlP light-emitting diode structures by optical overstress experiments under reverse bias

Cite as: J. Appl. Phys. **114**, 223106 (2013); <https://doi.org/10.1063/1.4848035>

Submitted: 24 October 2013 • Accepted: 01 December 2013 • Published Online: 12 December 2013

C. Karl, J. Ebbecke, R. Zeisel, et al.



View Online



Export Citation



CrossMark

## ARTICLES YOU MAY BE INTERESTED IN

[Interplay of different photoluminescence degradation mechanisms in InGaAlP light emitting diode structures investigated by intense laser excitation](#)

Journal of Applied Physics **114**, 033108 (2013); <https://doi.org/10.1063/1.4815875>

[High-efficiency InGaAlP/GaAs visible light-emitting diodes](#)

Applied Physics Letters **58**, 1010 (1991); <https://doi.org/10.1063/1.104407>

[Hydrogen passivation effects in InGaAlP and InGaP](#)

Journal of Applied Physics **76**, 7390 (1994); <https://doi.org/10.1063/1.357964>



Applied Physics  
Reviews

Read. Cite. Publish. Repeat.

19.162

2020 IMPACT FACTOR\*

# Unravelling concurring degradation mechanisms in InGaAlP light-emitting diode structures by optical overstress experiments under reverse bias

C. Karl,<sup>1</sup> J. Ebbecke,<sup>1</sup> R. Zeisel,<sup>1</sup> and A. Wixforth<sup>2</sup>

<sup>1</sup>OSRAM Opto Semiconductors, 93055 Regensburg, Germany

<sup>2</sup>Experimental Physics I, University of Augsburg, 86159 Augsburg, Germany

(Received 24 October 2013; accepted 1 December 2013; published online 12 December 2013)

We examine the influence of an applied reverse bias on the optically induced and measured photoluminescence degradation characteristics of an InGaAlP light-emitting diode (LED) structure. We show that a reverse bias applied simultaneously to laser excitation of the sample has a strong impact on the observable photoluminescence degradation properties of the structure investigated via intense laser excitation. With the help of this approach, it is possible to control the carrier density and the internal electric field of the diode independently. By doing this, a distinction of several usually interfering photoluminescence degradation mechanisms from each other is achievable. Further, a comparison of the experimental data with simulated data delivers some indication on the local origin of the defect evolution processes within the light-emitting diode structure. © 2013 AIP Publishing LLC. [<http://dx.doi.org/10.1063/1.4848035>]

## I. INTRODUCTION

In the past decades, light emitting diodes underwent a rapid development in efficiency and, therefore, already replace conventional light bulbs in many applications by now. Ever since the beginning of the development of light emitting diodes, the study and understanding of their degradation properties have been an important issue concomitant to progression and improvement concerning their efficiency. Especially, for the InGaAlP material system degradation is a quite complex topic and many years of research have been done in the scientific community in order to understand this degradation.<sup>1,2</sup> It is generally assumed that the reason for the degradation of semiconductor devices lies in the generation and annealing of different kinds of defects within the semiconductor material.<sup>3–6</sup> Nevertheless, many details of the physics behind InGaAlP-light-emitting diode (LED) degradation are still unrevealed. The reason for this lies in the fact, that one is confronted with several competing degradation paths in the semiconductor material itself, even if further influence due to metal contact and package degradation is ignored, which is a quite common phenomenon in semiconductor degradation.<sup>7</sup> These different degradation mechanisms progress simultaneously in the semiconductor crystal, when operating the device, each with individual characteristic time constants.<sup>3,8,9</sup> These time constants are dependent on the number of excited carriers during performance of an overstress experiment.<sup>10</sup> Furthermore, it is a quite common observable phenomenon in electrical overstress experiments that the particular degradation mechanisms affect the  $I$ - $V$  characteristics of a LED differently: some are more pronounced for smaller currents whereas others dominate for larger currents.<sup>2,11</sup> Apart from these well known  $I$ - $V$  dependences under electric operation of the device, similar dependencies of the photoluminescence degradation behavior on the excitation density in optical overstress experiments under intense laser excitation can be observed. It has been considered that this spreading of the photoluminescence degradation

behavior associated with the excitation density originates from excitation density related changes in the probed volume of the sample or, to be precise, from changes in the contribution of different quantum wells of the active region to the total photoluminescence signal.<sup>10</sup>

Such fluctuations of the carrier distribution and, therefore, also of the radiative recombination rate should be sensitive to an additionally applied electric field during optical excitation of the sample.

## II. SAMPLE AND EXPERIMENTAL SETUP

To pursue this idea, we here use this principally contactless optical degradation technique to test the photoluminescence degradation of the pure epitaxial LED material. The experimental setup and the principal of this technique have been described in a recent publication.<sup>10</sup> Nevertheless, in this work, an additional transparent indium tin oxide (ITO) contact layer is sputtered onto the sample surface as we want to investigate the influence of an additionally applied electric field on the optically induced degradation properties of the sample. The application of the transparent ITO contact onto the sample surface seems not to affect the photoluminescence degradation properties of the sample, as the photoluminescence degradation properties of the sample before and after the application of the ITO contact layer are equal. The idea of preferentially probing distinct defect types and their distribution across the LED test structure by a laser excitation density and electric field dependent inhomogeneous distribution of the radiative recombination rate is illustrated in Figure 1. The investigated sample is a metal organic vapor phase epitaxy (MOVPE) grown LED test structure with an undoped  $(\text{Al}_x\text{Ga}_{1-x})_{0.5}\text{In}_{0.5}\text{P}$  multiple quantum well (MQW) active layer and an emission wavelength of 588 nm at room temperature. The superlattice has a total thickness of about  $1.2\ \mu\text{m}$  and consists of 100 quantum wells and barriers. It is embedded between two doped  $(\text{Al}_x\text{Ga}_{1-x})_{0.5}\text{In}_{0.5}\text{P}$  confinement layers. In addition, the sample is covered with a 85 nm

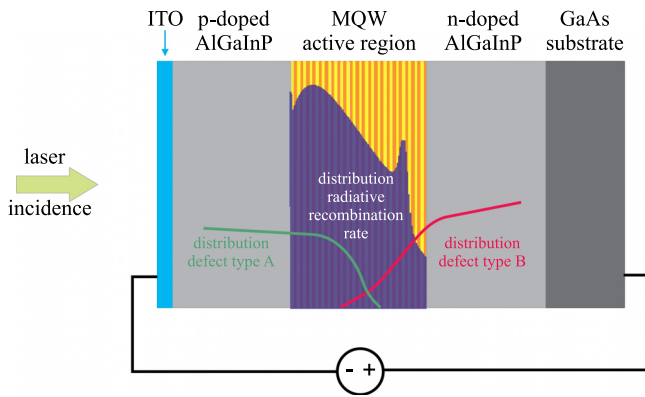


FIG. 1. Schematic sketch of the setup for probing distinct defect distributions by a laser excitation density and electric field dependent inhomogeneous distribution of the radiative recombination rate.

thick sputtered transparent indium tin oxide contact layer. As a back contact, the n-doped GaAs substrate is used.

The accelerated PL degradation experiments under intense laser excitation on the LED structure in our photoluminescence setup are carried out with the help of a frequency doubled diode pumped solid state laser emitting at a wavelength of 532 nm with a maximum output power of 750 mW. The electron hole pairs are excited resonantly within the MQW active region of the LED structure. The beam is focused to a spot of approximately 50  $\mu\text{m}$  in diameter at the sample surface. The sample is stressed for 18 h in total. After certain time intervals, the stressing of the sample is interrupted and the photoluminescence signal at the stressed point of the sample is recorded for a series of different measurement laser intensities. The measurement pulses are in the order of several ms to keep heating effects little. Additionally, a bias can be applied on the sample during measuring the degradation related change in photoluminescence intensity or during optical stressing of the sample, respectively.

### III. EXPERIMENTAL RESULTS

Figure 2 indicates the initial situation of the typical interplay of three distinct degradation mechanisms in a short

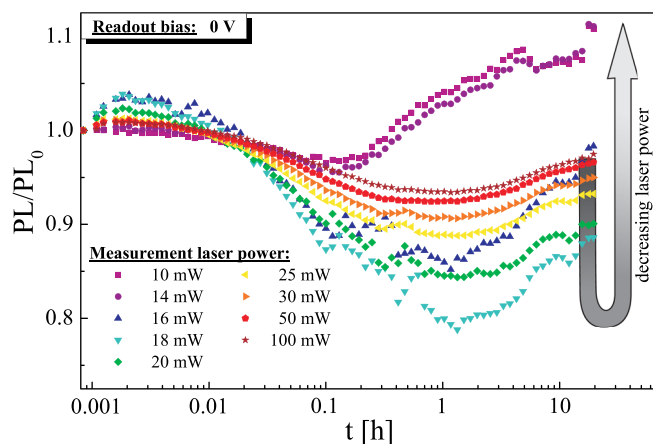


FIG. 2. Interplay of different degradation mechanisms for zero additional readout-bias depicted for a series of varying measurement laser intensities. The sample was stressed with a laser power of 400 mW and an excitation wavelength of 532 nm.

wavelength emitting InGaAlP LED structure without additionally biasing the sample. Three different degradation mechanisms can be identified. First of all, the sample shows an increase in photoluminescence intensity within the first few seconds of the degradation experiment. This initial phase of increase in PL intensity will be referred to as initial positive aging or initial positive degradation in the following. This positive initial aging is followed by a phase, where total degradation behavior is dominated by a negative aging mechanism and so the PL intensity is again decreasing with stressing time. Thus, this phase of decreasing photoluminescence intensity will be labeled as negative aging or degradation. However, on the long timescale, again an increase in the photoluminescence intensity can be seen, which counteracts the negative aging mechanism. This mechanism will be referred to as long term positive aging. The relative intensities of the three different aging mechanisms are dependent on the detection laser intensity used for investigation of the optically induced degradation of the sample for zero additional readout bias, as has been discussed in detail in a recent publication.<sup>10</sup>

#### A. Variation of readout bias

Figure 3 shows the influence of an applied readout bias  $U_{\text{readout}}$  on the detected degradation behavior, whereas the stress laser intensity (400 mW) as well as the measurement laser intensity (50 mW) are kept constant and no bias during stressing of the sample is applied. In the case of  $U_{\text{readout}} = 0$  V, the sample shows the known interplay of three different degradation components proceeding simultaneously with individual time constants as described in a recent publication.<sup>10</sup> The application of a reverse readout bias to the light emitting diode while recording the relative change in internal quantum efficiency  $\text{PL}/\text{PL}_0$  reveals a large impact on the observed degradation behavior. When increasing the reverse readout bias, first the negative aging mechanism becomes more and more dominant reaching its maximal strength for a reverse readout bias of  $U_{\text{readout}} = -1.5$  V, where no

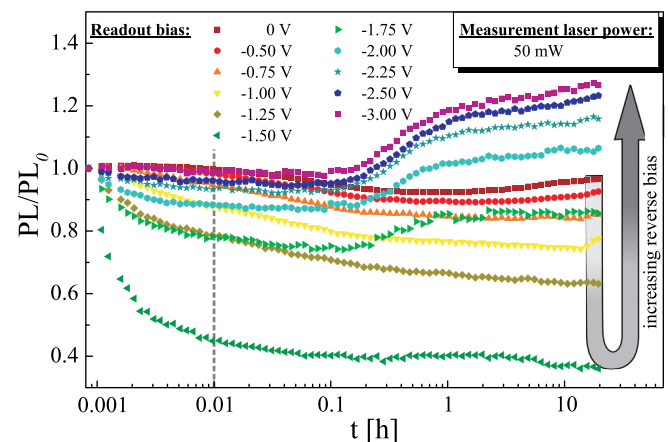


FIG. 3. Change of the degradation behavior with applied readout bias. The bias is applied while recording the photoluminescence signal during an optical overstress experiment. The sample was stressed with a laser power of 400 mW and an excitation wavelength of 532 nm. The photoluminescence degradation is measured for a laser power of 50 mW.

contribution of the initial positive aging and the long term positive aging components can be seen. Further, raising the reverse bias reduces the influence of the negative aging mechanism. At the same time, the positive long term aging mechanism is enhanced and eventually dominates the total degradation characteristics for large reverse bias. This change from an initial relative homogeneous interplay of all of the three degradation mechanisms to a totally dominating negative contribution and further reaching a prevailing strong positive aging mechanism when increasing the reverse readout bias is depicted by the arrow in Figure 3. Note that this behavior is quite similar, even though much more pronounced (compare different scales on the ordinates of Figures 3 and 2, respectively), to the change in the relative weighting of the different degradation mechanisms, which can be observed, when varying the exciting laser intensity under constant readout bias. This case is depicted by the arrow in Figure 2.

These degradation experiments under applied reverse readout bias, as exemplarily described above for a single measurement laser intensity of 50 mW, are performed for a series of different measurement laser intensities, while the stressing conditions of the sample are always kept constant. For a variation of the detection laser intensity in principal the same dependence of the degradation behavior on the applied readout bias can be observed for each of the distinct excitation densities. The difference consists in the fact that for increasing detection laser intensity, the point where the observed degradation behavior turns into a complete negative one shifts to larger values of the applied reverse readout bias- or, put in another way: to observe the phenomenon of complete negative aging for higher laser excitation intensities also a larger reverse readout bias is needed. So, the effects of increasing reverse bias and increasing laser intensity are counteracting. Figure 4 shows this dependence on the applied readout bias for several excitation densities of the sample. The graph depicts the relative change in the photoluminescence signal  $PL/PL_0$  measured after the sample was stressed for 0.01 h (dashed line in Figure 3).

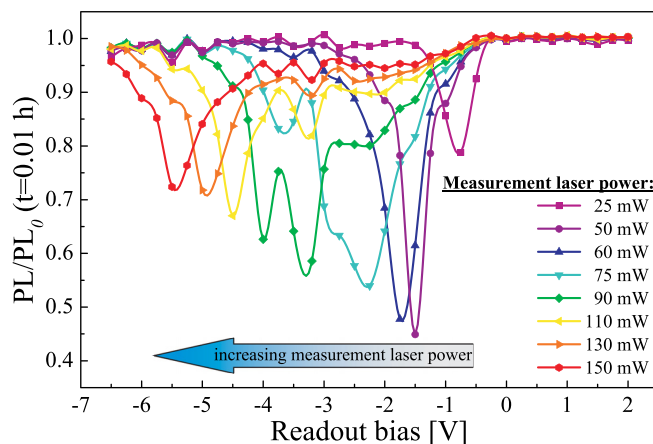


FIG. 4.  $PL/PL_0(t=0.01 \text{ h})$  as a function of the readout bias applied to the sample. The data are recorded for a series of different detection laser intensities. For higher excitation densities, the negative contribution to the degradation behavior becomes apparent only for larger values of reverse readout-bias.

Additionally, Figure 4 shows that for approaching the flat band condition when applying a readout bias in forward direction of the light emitting diode (but still remaining below the threshold voltage), the strong spreading of the degradation behavior for different measurement laser intensities vanishes. This issue has already been raised above, when discussing the different scales of the ordinates of Figures 2 and 3. There it could be seen that the variations in degradation dependencies for different measurement laser intensities occur on a much smaller scale in the unbiased case than under biased conditions.

## B. Variation of stress bias

It has been demonstrated above that it is possible to preferentially probe different degradation mechanisms by applying a reverse readout bias while measuring the photoluminescence degradation behavior of the sample. As a cross check, we also tried to trigger distinct degradation mechanisms selectively. Therefore, we performed PL degradation experiments where we applied a reverse stress bias on the sample while stressing it with high laser power density. No reverse readout bias was applied during recording the change in photoluminescence intensity. Figure 5 shows the PL degradation behavior of the sample for a series of different reverse stress biases for a constant stress laser intensity of 400 mW and a constant measurement laser intensity of 20 mW.

In analogy to the PL degradation experiments under reverse readout bias, the experimental data obtained under reverse stress bias reveal an enhancement of the negative aging component for increasing reverse bias. For a reverse stress bias  $U_{\text{stress}} = -6.0 \text{ V}$ , the defect growth process causing the negative photoluminescence degradation component dominates the total aging behavior and suppresses other defect evolution mechanisms almost completely. Further, increasing the reverse stress bias reinforces the positive long term aging mechanism concomitant to a reduction of the negative degradation process. Note that for triggering the negative aging mechanism while stressing the sample with

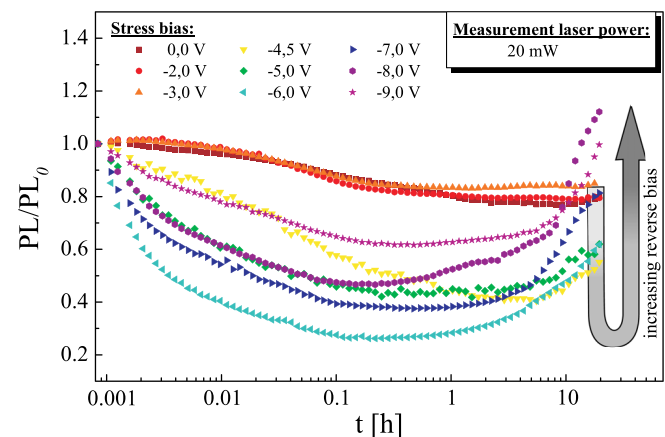


FIG. 5. Shift of the photoluminescence degradation behavior for several additionally applied reverse stress biases during stressing the sample with a laser intensity of 400 mW. The measurement laser intensity is kept constant and no readout bias is applied.

high laser power of 400 mW, a much larger reverse bias is needed compared to the probing experiments, where smaller laser intensities are used for the investigation of the photoluminescence degradation behavior, as the effects of laser excitation and reverse bias are counteracting with regard to their influence on the distribution of the radiative recombination rate within the LED structure, which is depicted in Figure 6.

#### IV. DISCUSSION

The dependence of the degradation behavior on the excitation intensity as well as its controllability via an additional applied bias on the sample indicates that optically induced electric field domains<sup>12</sup> and therewith related inhomogeneities in the distribution of the radiative recombination rate across the active region of the LED structure, as it is shown

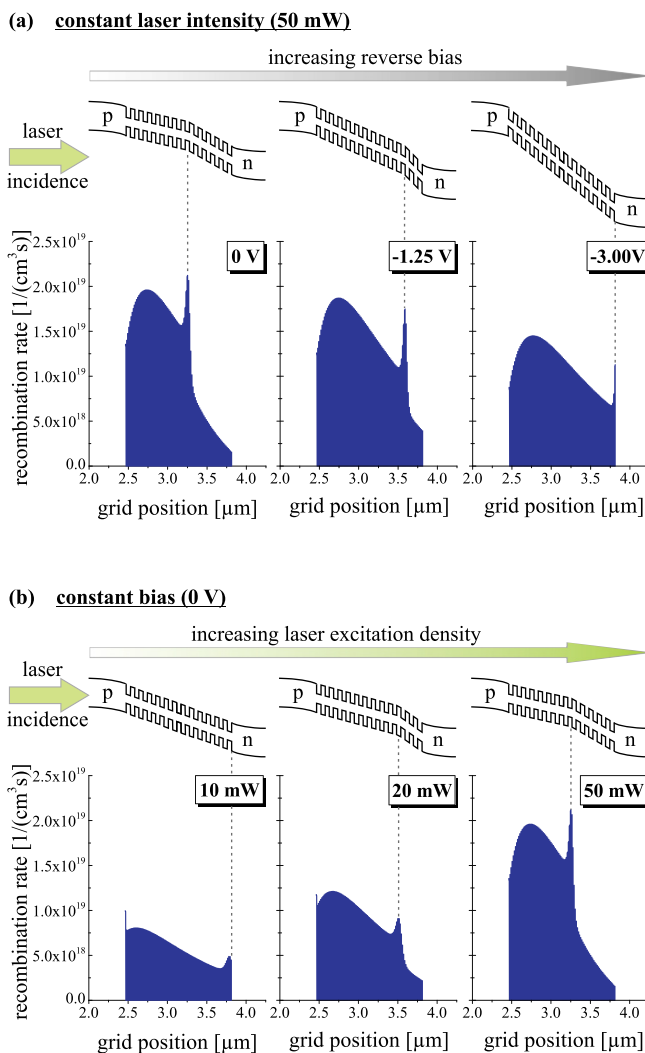


FIG. 6. Simulated distribution of the radiative recombination rate across the active region of the LED sample for different applied biases. The laser incidence is from the p-doped side of the sample. Figure (a) shows the dependence of the distribution of the radiative recombination rate in the case of constant laser excitation intensity and varying reverse bias. The incidence laser intensity used for the simulation corresponds to the excitation intensity at 50 mW in the experiment. Figure (b) depicts the simulation results for the case of constant bias  $U = 0$  V and varying laser excitation density. The peaks in the recombination rates are attributed to the boundary between different field domains within the superlattice.

in Figure 6, might be the explanation for the spreading of the photoluminescence degradation behavior with excitation laser power. This inhomogeneous distribution of the radiative recombination rate shifts with varying laser intensity and varying bias, respectively. In a recent publication, Shim *et al.* also suggested the possibility of a current dependent shift of the mean position of recombination for InGaAlP-LEDs under electric current.<sup>13</sup> In our case, we treat the case of optical excitation of an InGaAlP-LED structure.

Figure 6 shows the simulated inhomogeneous distribution of the radiative recombination rate for varying bias under constant laser excitation and for varying laser intensity under constant bias, respectively. The simulations are performed employing SimWindows and the simulation parameters are corresponding to the experimental conditions. The simulated distribution of the radiative recombination rate depicted in Figure 6(a) shows the case of constant laser excitation intensity under reverse bias and, therefore, corresponds to the experimental degradation data shown in Figure 3. For an applied bias of  $U = 0$  V, an inhomogeneous distribution of the radiative recombination rate across the active region of the LED structure can be seen with a dominating contribution of the p-sided quantum wells to the total photoluminescence signal. Therefore also defect evolution processes affecting the p-sided quantum wells should be the dominating mechanism which can be observed in optical overstress experiments. Increasing the reverse bias also the n-sided quantum wells contribute more and more to the total photoluminescence signal leading to an increasing influence of degradation mechanisms located at the n-side of the active region to the total degradation behavior. The peak of the recombination rate is correlated to the boundary between high and low field domain. This boundary shifts across the superlattice for varying additional bias. The situation depicted in Figure 6(b) is just vice versa; here, the bias is kept constant at  $U = 0$  V and the intensity of the exciting laser is varied. This case corresponds to our experimental data presented in Figure 2.

As has been mentioned before, when discussing the experimental data, the experimentally observed degradation in the case of constant bias and varying measurement laser intensity behaves quite similar but vice versa as in the case of constant laser excitation and increasing bias. This issue is indicated by the arrows in Figures 2 and 3, respectively. So, the long term positive degradation mechanism becomes dominant for *decreasing* laser intensity in contrast to its enhancement with *increasing* reverse bias. This is in perfect agreement with our simulation results for the distribution of the radiative recombination rate shown in Figure 6(b): the relative contribution of the n-sided quantum wells to the total photoluminescence signal decreases with increasing excitation intensity. A comparison of Figures 6(a) and 6(b) emphasizes the counteracting effect of increasing reverse bias and laser excitation intensity on the distribution of the radiative recombination rate, which is also reflected by our experimental data.

Assuming different types of defects with different annealing and growing properties being located rather at the p-side of the active region or at the n-side, it becomes apparent that with varying laser excitation densities and bias, the

detected photoluminescence signal of the sample is dominated by defect evolution processes originating from different locations within the LED structure.

## V. CONCLUSION

In conclusion, we demonstrated that optical degradation experiments under additionally applied bias provide an opportunity for gathering further information on the degradation properties of LED structures. With the help of this approach, it is possible to vary the carrier density within the sample on the one hand and manipulate the internal electric field of the diode on the other hand independently from each other. This cannot be achieved when operating the LED under electric current conditions as there the carrier density within the sample is always linked to the changes within the built in electric field. By taking advantage of this additional degree of freedom, it becomes possible to unravel the usually observable superposition of different degradation mechanisms and even to associate particular degradation mechanisms to potential sites of origin within the LED structure.

- <sup>1</sup>P. Altieri-Weimar, A. Jaeger, T. Lutz, P. Stauss, K. Streubel, K. Thonke, and R. Sauer, *J. Mater. Sci.: Mater. Electron.* **19**, 338 (2008).
- <sup>2</sup>O. Pursiainen, N. Linder, A. Jaeger, R. Oberschmid, and K. Streubel, *Appl. Phys. Lett.* **79**, 2895 (2001).
- <sup>3</sup>A. Khan, M. Yamaguchi, J. C. Bourgoin, K. Ando, and T. Takamoto, *J. Appl. Phys.* **89**, 4263 (2001).
- <sup>4</sup>Y. Horikoshi, T. Kobayashi, and Y. Furukawa, *Jpn. J. Appl. Phys.* **18**, 2237 (1979).
- <sup>5</sup>J. Dekker, A. Tukiainen, N. Xiang, S. Orsila, M. Saarinen, M. Toivonen, M. Pessa, N. Tkachenko, and H. Lemmetyinen, *J. Appl. Phys.* **86**, 3709 (1999).
- <sup>6</sup>D. V. Lang, *Annu. Rev. Mater. Sci.* **12**, 377 (1982).
- <sup>7</sup>C. L. Zipfel, R. H. Saul, A. K. Chin, and V. G. Keramidas, *J. Appl. Phys.* **53**, 1781 (1982).
- <sup>8</sup>S. K. K. Lam, R. E. Mallard, and D. T. Cassidy, *J. Appl. Phys.* **94**, 1803 (2003).
- <sup>9</sup>S. K. K. Lam, R. E. Mallard, and D. T. Cassidy, *J. Appl. Phys.* **95**, 2264 (2004).
- <sup>10</sup>C. Karl, J. Ebbecke, T. Lutz, C. Kaus, and R. Zeisel, *J. Appl. Phys.* **114**, 033108 (2013).
- <sup>11</sup>J. M. Ralston and J. W. Mann, *J. Appl. Phys.* **50**, 3630 (1979).
- <sup>12</sup>H. T. Grahn, H. Schneider, and K. von Klitzing, *Phys. Rev. B* **41**, 2890 (1990).
- <sup>13</sup>J.-I. Shim, D.-P. Han, H. Kim, D.-S. Shin, G.-B. Lin, D. S. Meyaard, Q. Shan, J. Cho, E. F. Schubert, H. Shim, and C. Sone, *Appl. Phys. Lett.* **100**, 111106 (2012).